

AN INTERNATIONAL ACCELERATOR FACILITY FOR BEAMS OF IONS AND ANTIPROTONS, PLANS AND R&D

N. Angert, B. Franzke, P. Spiller, K. Beckert, P. Beller, K. Blasche, O. Boine-Frankenheim, A. Dolinskii, G. Franchetti, B. Franczak, I. Hofmann, P. Hülsmann, K. Kaspar, A. Krämer, G. Moritz, E. Mustafin, F. Nolden, C. Peschke, H. Reich-Sprenger, P. Schütt, M. Steck
GSI, Planckstrasse 1, D-64291 Darmstadt, Germany

1 Overview to New Facility

The conceptual design report for an "International Accelerator Facility for Beams of Ions and Antiprotons" [1] on the GSI site was presented in autumn 2001. The proposal was evaluated in 2002 among other proposals for large-scale research instruments by the federal Research Council, which gave a fairly positive recommendation in favor of the GSI-proposal. In a press release of February 9, 2003, the federal research minister (BMBF) gave 'green light' for the preparation of the 675 M€ project a quarter of which has to be contributed by international partners. The proposed accelerator complex (see fig. 1) may be characterized by following major scientific objectives:

- Nuclear structure physics with rare isotope beams (RI beams) at high mean intensities for external target experiments and high peak intensities for internal target experiments with cooled beams of short-lived nuclei.
- Nuclear collision experiments investigating compressed baryonic matter with heavy projectiles up to $^{238}\text{U}^{92+}$ at specific projectile energies up to 34 GeV/u.
- Internal target experiments with cooled antiproton beams at luminosities up to $2 \times 10^{32} \text{ cm}^{-2} \text{ s}^{-1}$ for investigations of exotic hadronic states with high resolution.
- Atomic physics experiments with high-Z ions in a wide energy range up to relativistic energies.
- Plasma physics experiments investigating evolution and properties of hot, dense plasmas generated by means of intense heavy ion beam pulses.

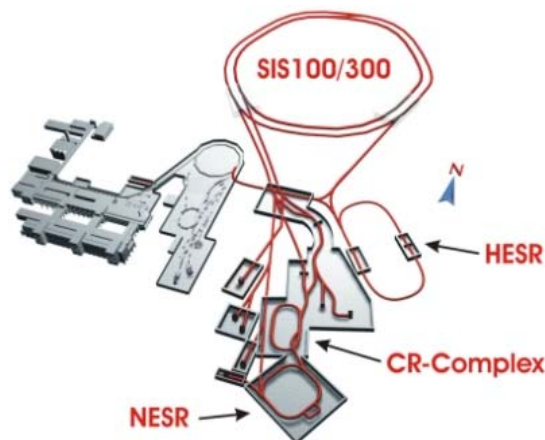


Figure 1: Preliminary layout of the proposed accelerator/storage ring facility at GSI (see text below).

The layout of the proposed accelerator/storage ring complex is shown in figure 1. The existing UNILAC-SIS18 accelerators (left side) shall serve as injectors, supplemented by a 50 MeV proton linac for antiproton production. The fast-cycling 100 Tm-synchrotron SIS100 [2], equipped with super-ferric 2 T-dipoles (ramp rate 4 T/s), will accelerate 1×10^{12} U^{28+} -ions per cycle for RI production at 1-2.7 GeV/u and 2×10^{13} protons per cycle for antiproton production at 29 GeV. The high beam intensities per SIS100 cycle are obtained by means of multi-turn filling the SIS18 up to the space charge limit at injection energy (11.5 MeV/u for heavy ions and 50 MeV for protons) and by accumulating 4 to 5 SIS18 cycles in the correspondingly larger SIS100 ring. The super-conducting 300 Tm-SIS300, installed in the same ring tunnel, will be used to accelerate about 1×10^{10} U^{92+} -ions up to 34 GeV/u for nuclear collision experiments, but alternatively also as stretcher for SIS100-beams.

2 The Linac Injector Concept

The new facility builds for heavy ions on the existing heavy ion accelerator UNILAC. It will provide beams of up to 12.5 mA of U^{28+} at 11.4 MeV/u to the SIS18. To achieve that, the UNILAC prestripper accelerator (Wideröe type) has been replaced in 1999 by a new RFQ and IH structure which is capable to accelerate 15 mA of U^{4+} up to 1.4 MeV/u. There stripping takes place in a supersonic gas jet. This new high current prestripper linac is, however, not suited for high proton currents. Therefore, for the new facility an additional proton linac has to be built for 50 MeV 50 mA proton beams.

2.1 UNILAC Upgrade

The UNILAC main accelerator (1.4 to 11.4 MeV/u) has two injector linacs. The first one, the high current prestripper linac, is equipped with high current ion sources of MEVVA and MUCIS type designed for low charge states. It allows acceleration of ions with a mass to charge ratio of 65. Currents of up to 30 mA of U^{4+} can be achieved with the MEVVA ion source. However, beam formation during the pre-acceleration to the injection energy of the RFQ of 2.2 kV/u is accompanied by large emittance growth due to the heavy space charge. Therefore, new pre-acceleration systems are under investigation to reduce emittance growth. In addition, matching to the RFQ and beam loss in the first section of the RFQ is still a major issue. The transmission of the RFQ is for high currents only around 60 %. That means that the first part of the RFQ has to be replaced as well as the matching optics to the RFQ according to new design considerations in order to reach the design currents of 15 mA for uranium. Up to 8 mA have been achieved so far with the new 36 MHz RFQ/IH linac at 1.4 MeV/u.

In parallel to the high current injector linac a high charge state injector linac with 108 MHz RFQ/IH structures and a 14 GHz ECR ion source is in operation. This ECR ion source provides the same charge states for uranium (28+) as is achieved after stripping at 1.4 MeV/u. New ECR source developments are under way in an international collaboration to provide U^{28+} currents in pulsed mode up to a few mA with superconducting magnet fields and a 28 GHz micro wave generator. That would improve intensities from the high charge injectors by at least one order of magnitude. Thereby, acceleration of different ion species could be also provided with high intensities for the new facilities. The option of accelerating different ion species for the different experimental programs proved extremely valuable in the existing facility.

2.2 New Proton Linac

The proton currents from the existing UNILAC are limited to a few mA. In order to achieve the currents needed for the antiproton program a separate proton linac has to be installed. It will consist of a 4-rod or 4-vane RFQ structure for a few MeV, followed by a CH-DTL structure for an output energy of 50 MeV. The design currents at 50 MeV are 50 mA with an emittance of 5 mm mrad. The new linac will be developed in cooperation with the Institute for Applied Physics at Frankfurt University [1]. The considered CH-structure has a rather high shunt impedance. Presently frequencies of 433 and 352 MHz are under consideration. The final choice will depend on the availability and cost of the RF-systems. Design studies of the particle dynamics and investigations of the RF-structure are presently being performed.

3 Synchrotron Design Concept

For the first new synchrotron stage SIS100 superconducting magnets of superferriic type were proposed to provide a moderate pulse power at a rather large aperture of 130 x 65 mm and an operation with one cycle per second. A cold beam tube is foreseen to obtain a sufficiently high pumping speed for a stable operation with intermediate charge-state heavy ion beams.

The bending magnets are arranged in six arcs. The six long straight sections in between provide space for injection and extraction, the transfer line from SIS100 to SIS300 and also for the RF-systems required for acceleration (300 kV) and fast bunch compression (1000 kV). Like in the SIS18 triplet focusing will be used to achieve a large acceptance at injection with dynamic change-over to doublet focusing during acceleration. Four SIS18 booster cycles will be used to fill the SIS100 with up to 2×10^{13} protons or 1×10^{12} U^{28+} ions.

For the production of radioactive ion (for storage ring experiments) and antiproton beams, the accelerated beam will be transformed into one single short bunch (about 50 ns for heavy ions). Thereby the produced secondary beams will have an appropriate time structure for injection, fast debunching and cooling in the planned array of cooler/storage rings. The SIS100 will be also used to accelerate cooled and accumulated antiproton beams from 3 GeV up to 14 GeV for experiments in the high energy storage ring HESR.

The second synchrotron stage SIS300, was planned with superconducting $\cos\theta$ -magnets for operation up to a flux density of 4 T. Meanwhile it is discussed to raise the flux density to 6 T by making use of double layer coils. The SIS300 ring will be both used for acceleration of U^{92+} -beams to high energies up to 34 GeV/u and as a stretcher ring to obtain a near to 100 % duty cycle linac-like beam in operation with slow extraction for fixed target experiments with rare isotope beams.

3.1 Superconducting Magnets

SIS100

Superconducting window-frame magnets shall be used in the SIS100 [3]. One major design goal was to achieve a low amount of stored energy, i.e. 45 kJ in a 2.62 m long dipole magnet with a beam tube aperture of 130 x 65 mm compared to 112 kJ in a conventional magnet as the one used in the SPS (CERN) or the SIS18 (GSI). Such a design reduces the total peak power of 120 magnets in fast pulse operation with a

ramp rate of 4 T/s, a repetition rate of 1Hz and a peak field of $B=2$ T to the moderate value of $+22/-22$ MVA compared to $+62/-50$ MVA in a conventional design. In addition, the magnet weight will be strongly reduced to about 2 t per magnet compared to 20 t for a conventional magnet. The magnet design is based on the superferric cold iron magnet, which has been used in the Nuclotron at the JINR Dubna since 1993. In close cooperation with the JINR the dynamic losses of the existing magnets could be reduced to a value of 18 W/m. This translates into total power losses of 5.4 kW at 4K for 120 dipole magnets using a standard triangular cycle (2T, 1Hz). In parallel an improvement of the field quality and the mechanical long-term stability was achieved. Figure 2 shows that the original losses of about 40 W/m have been reduced to 18 W/m.

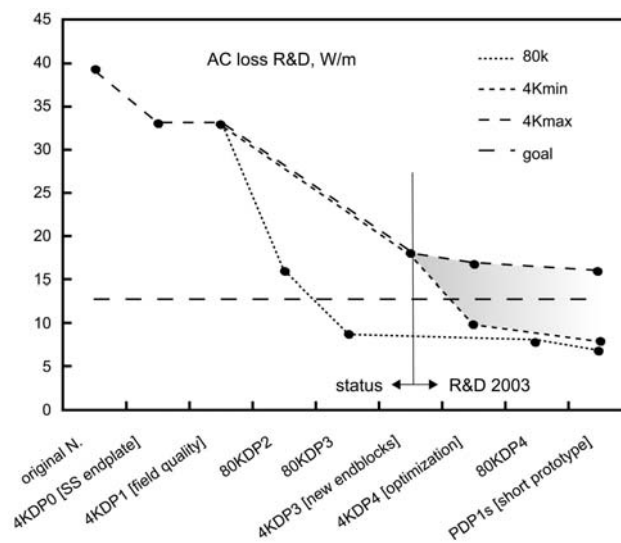


Figure 2 : A significant reduction of the dynamic losses of the Nuclotron magnet has been achieved through different development steps since begin 2000 (s. text).

To determine the sources of the losses, a detailed test program was launched. The 3D field configuration at the magnet ends was found to be one of the most important sources for eddy current losses in the iron yoke. 3D calculations confirmed the measured data [4].

In parallel, an alternative magnet design with an iron yoke at 80 K was developed and tested. The remaining AC loss in the coil amounts to 9 W/m (Figure 2) [5]. As an additional design option, the replacement of the Nuclotron cable by a CICC cable was studied [6]. The model magnet development for SIS100 shall be completed by the end of 2004.

SIS300

The SIS300 will be equipped with superconducting magnets similar to the RHIC arc dipole (BNL) with a one-layer $\cos\theta$ -coil, or the UNK dipole (IHEP) with a two-layer coil. In cooperation with BNL, a RHIC dipole was modified to reduce the dynamic losses for a standard triangular cycle (4 T, 1/8 Hz). Tests of a first model dipole started at the end of 2002. With the main emphasis on the development of a cored Rutherford cable dynamic losses of 9 W/m were achieved [7]. This translates into a total power loss of 2.8 kW at 4K for 120 dipole magnets.

There is a strong user interest in raising the maximum beam energy of the second synchrotron stage by using 6 T dipole magnets for an operation of up to $B_p=300$ Tm.

In cooperation with IHEP the design of the 6 T UNK dipole magnet, constructed with a two-layer $\cos\theta$ -coil has been modified for operation at a fast ramp rate of 1T/s [8]. Planned R&D to achieve this goal will include a large coil inner radius of 100 mm, an increase of the temperature margin and tests of model magnets.

3.2 RF Systems

The planned SIS100 operation requires powerful low-frequency RF systems for stacking, acceleration and bunch compression. A low bunching factor is required in order to restrict the space charge tune shift to $dQ < 0.2$ during the long injection time of 1s. Bunching factors of 0.45 and 0.85 can be achieved in a multi-harmonic and a barrier bucket potential. Both options are presently under investigation.

Acceleration in SIS100 at $h=10$ requires a total RF voltage of 290 kV in a frequency range of 1.1-2.8 MHz. Generation of short, single bunches after acceleration needs 1 MV of compression voltage at the extremely low frequency of 465 kHz.

Two alternative concepts for the technical layout of the RF systems are being investigated. The first option is to install two separate RF systems for acceleration and compression, while the second option is to combine both functions in the same RF system [9]. Detailed design studies and optimisations with respect to costs, peak power requirements, shunt impedance and maintainability are in progress.

Table 1 : Comparison between separated and combined RF systems for acceleration and compression. $V_{0,a}$ and $V_{0,c}$ are the gap voltages of the acceleration and compression systems, $N_{a,c}$ the total number of cavities, $L_{a,c}$ the total RF system length and P_c the peak power of the compression system.

	$V_{0,a}$	$V_{0,c}$	$N_{a,c}$	$L_{a,c}$	P_c
Separate RF Systems	16kV	40kV	18+25	57m +21m	20MW
Combined RF System	3Kv	10kV	100	90m	10MW

The SIS300 RF system consists only of acceleration cavities which will provide a total voltage of 80 kV.

3.3 Dynamic Vacuum and Beam Life Time

Measurements in the SIS18 showed that the stripping cross section σ for U^{28+} at 8.6 MeV/u is of the order of 10^{-16} cm^{-2} . With increasing energy the observed beam lifetime does not improve. From that one can conclude that the product σI (current I) remains constant under the present SIS18 UHV conditions [10]. In order to limit the beam losses due to stripping in the residual gas to values below a few percent a pressure in the 10^{-12} mbar region must be ensured in all (warm and cold) sections of SIS 100/300. Recent experiments at CERN, BNL and GSI showed that lost heavy ions in the energy range between 1 and 10 MeV/u lead to large outgassing rates of heavy gas components from stainless steel chambers. The measured desorption coefficient η varies for different materials, ion species, and energies between 10^3 and 10^5 molecules per incident beam ion. Assuming homogenously distributed stripping losses and pumping, the equilibrium dynamic pressure is

$$P = \frac{P_0}{1 - \frac{L}{S} \eta \sigma \frac{I}{q}}$$

with the pumping speed S , the base pressure $P_0 = Q/S$ (thermal outgassing rate Q), the circumference L and the beam current divided by the charge I/q . Using the existing pumping speeds in SIS18 ($S/L \approx 70 \text{ l m}^{-1}\text{s}^{-1}$) together with the measured parameters we obtain a negative denominator, meaning a pressure instability, for the SIS100 design current at injection energy. In agreement with analytic theory the pressure instability was observed in the SIS18 at relatively low ($N \approx 10^9$) uranium intensities, however, with a high fraction (about 20%) of heavy gas components like H_2O , CO , Ar . In order to maintain the required pressure of 10^{-12} mbar in the warm sections of SIS100/300 ongoing efforts focus on low- η materials for e.g. collimators, on combined collimator/pumping posts and on increased linear pumping in NEG coated chambers. All these measures should reduce the ratio η/S by a factor 1/1000 compared to the existing SIS18. In the cold sections the cold wall pumping ($S/L \approx 10000 \text{ l m}^{-1}\text{s}^{-1}$) needs to be confirmed for the SIS100/300 environment [11]. Such efficient pumping is hoped to limit the dynamic pressure increase in the cold sections.

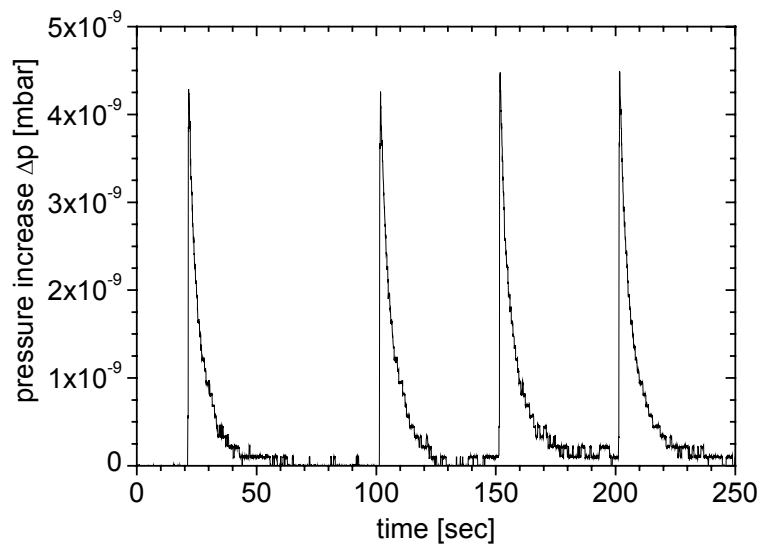


Figure 3 : Measured beam-desorption induced total pressure increase in GSI the test-stand. Shown is the pressure rise by the irradiation of a Cu sample with a 1.4 MeV/u C^{2+} -beam (single shot 50 μA , 5 ms).

In order to measure the scaling of the desorption coefficient with projectile energy, mass and charge, a desorption test-stand was recently set-up at GSI. These experiments should also help to find low- η materials suitable for collimators or for vacuum chambers. First results with low energy (1.4MeV/u) C^{2+} -ions irradiating a Cu target are shown in Figure 2.

The distribution of losses due to ionisation of U^{28+} to U^{29+} and the thereby deposited energy per meter have been determined for the SIS100 lattice. The losses occur mainly after charge separation in the arc dipoles. Figure 4 shows the calculated energy distribution assuming a fraction of 5% lost ions. The plot shows the strongly peaked energy deposition along the beam pipe with a maximum after the first pair of dipoles following the straight sections.

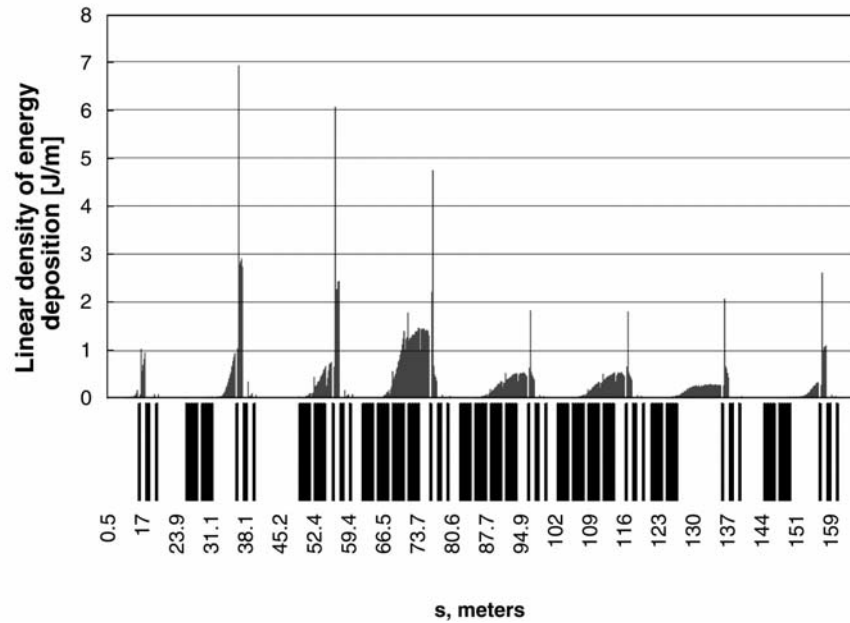


Figure 4: Calculated distribution of beam loss induced energy deposition in one arc of SIS100, assuming 5% losses of the initially 10^{12} U^{28+} ions.

One option to act against the vacuum instability is to control as many as possible of the lost ions by installing new type of collimators in the hot spots. Basis for this counter measure is the assumption that the threshold for vacuum instability can be enhanced if the ion loss-induced heavy gas molecules are to a large fraction prevented from reaching the optical axis. Therefore, a prototype of desorption collimator was developed for the U^{28+} -operation and will be tested in SIS18 [12]. The concept of the proposed collimator is to localize beam losses and to capture the desorbed gases in a secondary vacuum chamber (Figure 5). A wedge shaped block acts as an asymmetric beam scraper for higher charge states. It is installed such that the surfaces points to contrary direction of the optical axis. In order to eliminate the desorbed gases produced on the wedge surface, the secondary chamber is equipped with two high conductivity pumping ports and with a powerful cryopumping system. First tests of the prototype desorption collimator are planned for August 2003.

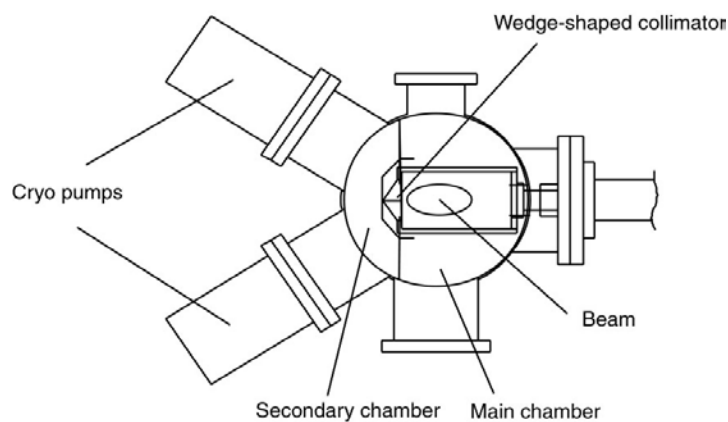


Figure 5: Layout of a dedicated collimator for the control of ionisation beam losses and desorbed gases.

4 Secondary Beam Production

4.1 Rare Isotope Beams

Experimental data measured at the existing fragments separator FRS behind SIS18 confirmed that optimal yields of neutron-rich, i.e. most exotic, nuclei are obtained by induced fission of ^{238}U -projectiles at energies up to 1.5 GeV/u. Therefore, ^{238}U may be considered as reference nucleus for the formation of rare isotope ion beams at the proposed facility. The acceleration of $^{238}\text{U}^{28+}$ ions in the proposed SIS18-SIS100 accelerator combination will allow not only to attain a high primary beam intensity of 1×10^{12} ions per cycle, but also to compress all projectiles into a single bunch of only 50 ns duration and 2% full momentum spread. The concept of time focusing minimizes the increase of the longitudinal emittance for the secondary beams and makes it possible to apply fast de-bunching (i.e. fast momentum spread reduction) after injection to the CR.

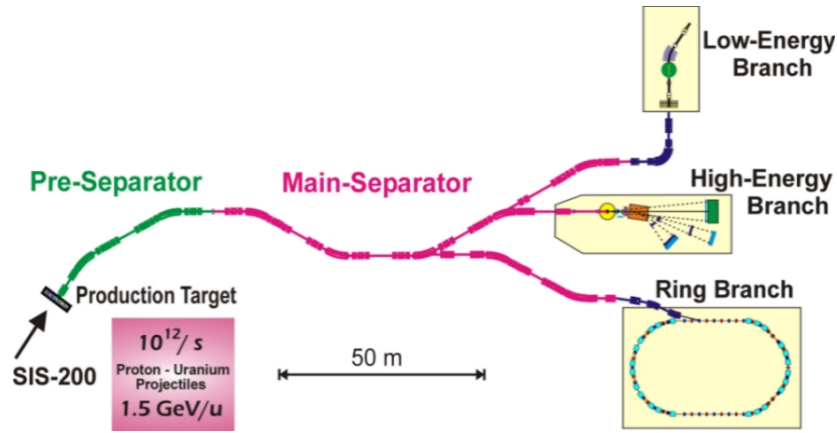


Figure 6: Layout of the Super-FRS [13], a magnetic separator equipped with super-ferric dipole and quadrupole magnets. The maximum bending power $B \times \rho_{\max}$ is 20 Tm, the resolving power $M/\Delta M$ about 1500.

Table 2: A few examples of expected RI intensities per SIS100 cycle after Super-FRS and injection to the CR. The heavy species are produced by induced fission of 1×10^{12} uranium projectiles per cycle at 1.5 GeV/u, the lighter ones by fragmentation of lighter projectiles (e.g. ^{55}Ni from ^{58}Ni) at lower specific energies. Decay times are given for nuclei at rest [13].

Nucleus	Yield / cycle	Decay time $\tau_{1/2}$ [s]
$^{11}\text{Be}^{4+}$	6.0×10^8	13.8
$^{46}\text{Ar}^{18+}$	3.2×10^8	7.8
$^{55}\text{Ni}^{28+}$	3.9×10^7	0.2
$^{71}\text{Ni}^{28+}$	6.7×10^6	2.6
$^{91}\text{Kr}^{36+}$	4.2×10^7	8.6
$^{104}\text{Sn}^{50+}$	5.0×10^5	20.8
$^{132}\text{Sn}^{50+}$	4.0×10^7	39.7
$^{133}\text{Sn}^{50+}$	4.0×10^6	1.4
$^{187}\text{Pb}^{82+}$	1.0×10^7	15.0
$^{207}\text{Fr}^{87+}$	3.2×10^7	14.8
$^{227}\text{U}^{92+}$	1.6×10^6	66

It should be mentioned that, by each beam bunch, a rather large fraction (up to 30%) of the total beam energy of about 57 kJ at 1.5 GeV/u is deposited in a small volume of

about 10 mm^3 in the (C, Al or Mg) production target of a few g cm^{-2} thickness. The power loss of 340 GW averaged over 50 ns will destroy every kind of conventional (solid) target by immediate melting and shock waves [14]. Therefore, the development of targets that can be renewed after each beam bunch (every second or even faster) is crucial.

4.2 Antiproton Beam

The bunching procedure described above is applied also to the proton beam for the antiproton production. The concept – kinetic energy of 29 GeV and intensity of 2×10^{13} primary protons, target and collection techniques, and acceptance of the CR (see Tab. 3) – is very similar to that of the former AAC-complex at CERN [15,16]. However, because of the higher proton intensity and energy, we expect a somewhat higher antiproton yield of 5×10^{-6} per incident proton at the desired energy of 3 GeV, i.e. about 1×10^8 per bunch.

5 Fast Cooling in CR Complex

The necessity of fast cooling and accumulation in the CR complex is determined by the consumption rates at the highest luminosities for the internal target experiments with the cooled secondary beams and, in the case of rare isotope beams, additionally by the decay time $\gamma \tau_{1/2}$ of the exotic nuclei in the laboratory system (see table 2).

Table 3: Selection of basic CR parameters.

Bending power	13 Tm		
Circumference	200.6 m		
Super periodicity	2		
Lattice type	FODO		
Operation modes	pbar cooling	RIB cooling	Isochr. mode
Maximum energy [GeV/u]	3	0.79	0.79
Betatron tunes Q_h	4.62	3.42	2.36
Q_v	4.19	3.36	3.36
Transition energy, γ_{tr}	4.3	2.88	1.84
Horiz. acceptance [μm]	240	200	70
Vertical acceptance [μm]	240	200	50
Momentum acceptance	$\pm 3\%$	$\pm 1.75\%$	$\pm 0.7\%$
Stoch. cooling at [GeV/u]	3	0.74	-
at $\beta=v/c$	0.97	0.84	-
at γ	4.2	1.8	1.84
Revol. frequency [MHz]	1.5	1.3	1.3
Frequency slip factor η	≤ 0.07	0.17	0.0
Rf peak amplitude [kV]	400	400	-
$\delta p/p$ after de-bunching	$\pm 0.6\%$	$\pm 0.35\%$	-

5.1 CR Lattice

The large acceptance Collector Ring CR (see table 3 and figure 7) is the first stage of the storage ring branch of the proposed facility [17]. Its maximum bending power of 13 Tm allows for the injection of rare isotope beams at 740 MeV/u and, reversing the polarity of all magnets, of antiproton beams at 3 GeV. Mainly due to the different particle velocities the ion optics has to be flexible in order to achieve optimum conditions for fast stochastic cooling for both species of beams (see table 3). In addition, the CR has to be operated in the isochronous mode ($\gamma = \gamma_t$) at a relatively low $\gamma_t = 1.84$ for time-of-flight mass spectrometry of exotic nuclei.

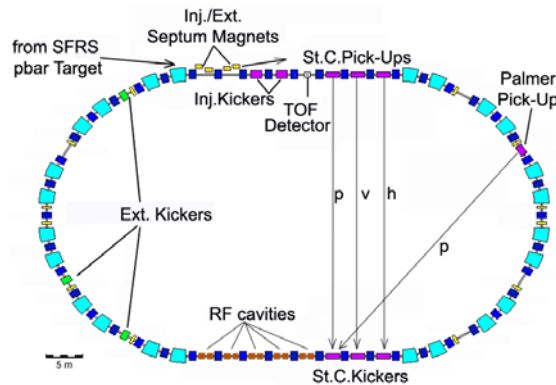


Figure 7: Layout of the Collector Ring CR. The ring will be equipped with superferriic dipole magnets. The Palmer pickup is necessary only for rare isotope beams at the beginning of momentum cooling (too strong unwanted mixing).

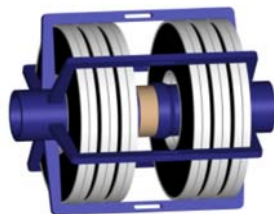
So far, two different lattice structures have been studied carefully: a lattice with identical ion optical settings in 180^0 -arcs and a so-called split ring lattice with strongly reduced frequency slip factor η in the arc between stochastic cooling pickups and kickers, which had been already proposed about 10 years ago for the Super-LEAR lattice [18]. The results of the studies for the split ring lattice in comparison with the symmetric lattice may be summarized as following:

- the number of quadrupole families is increased by nearly a factor of 2,
- chromaticity and higher order field corrections are much more complicated, and
- the dynamic apertures seem to be considerably smaller (if not too small) compared to the physical apertures.

Before the final decision about the choice of the CR lattice, numerical calculations of transverse cooling rates for all phases of the cooling process have to be completed.

5.2 Bunch Rotation

As explained above the injected secondary beam particles are concentrated in a single, 50 ns long beam bunch. This permits immediately after injection fast momentum spread reduction by a factor of approximately 5 by means of bunch rotation followed by



Load material	MA
Reson. RF for RI	1.3 MHz
Reson. RF for pbar	1.5 MHz
Voltage	40 kV _{pp}
Shunt impedance	929 Ω
Power	862 kW
Length	1 m

Figure 8: Preliminary layout and parameters of the CR bunch rotation cavity. 10 cavities are required.

adiabatic debunching. The first harmonic RF cavities have to be tuned to 1.3 MHz for RI beams and to 1.5 MHz for antiprotons. A rather high total RF voltage of 400 kV_{pp} is necessary in the case of RI bunches, for which a compromise between enough horizontal acceptance and sufficiently small frequency slip factor $\eta=0.17$ is much harder to find.

5.3 Stochastic Cooling

The starting conditions for stochastic cooling are determined by large transverse emittances and by the momentum spread after bunch rotation and adiabatic debunching. Because of the stronger (unwanted) mixing the momentum cooling of rare isotope beams starts with the so-called Palmer method until the momentum spread is below the mixing limit for notch filter cooling ($\delta p/p \approx \pm 0.1\%$). The Palmer pickup is installed at a position, where the dispersion amplitude is large compared to the betatron amplitude. The momentum deviation is deduced from the difference between signals from inner and outer electrodes of the pickup system. As the Schottky power is proportional to the square of the ionic charge Z , the high charge states of rare isotopes ($Z \geq 25$) guarantee an excellent signal to (thermal) noise ratio.

Table 4: Parameters for stochastic cooling at CR

		Pbar cooling	RI cooling
After injection	Horiz. emittance [μm]	240	200
	Vertical emittance [μm]	240	200
	Momentum spread [%]	± 3	± 1.75
After de- bunching	Horiz. emittance [μm]	240	200
	Vertical emittance [μm]	240	200
	Momentum spread [%]	± 0.5	± 0.35
After cooling	Horiz. emittance [μm]	0.5	5
	Vertical emittance [μm]	0.5	5
	Momentum spread [%]	± 0.1	± 0.05
Total cooling time [s]		5.0	0.5-1

Transverse cooling of antiprotons and rare isotopes will be switched on when the unwanted mixing between pickups and kickers has reached tolerable values and the wanted mixing between kickers and pickups is still strong enough. This is the case at a momentum spread of approximately $\pm 0.3\%$. This preliminary estimate has to be confirmed by numerical simulation of the cooling process. The corresponding computer code based on the Fokker-Planck approach is in preparation and should be available by the end of this year.

The preliminary technical layout of the stochastic cooling system at the CR is based on power-amplifiers for two or three bands in the frequency range 1 to 4 GHz. The 50 Ω -kickers will be equipped with a total power of about 8 kW. Mainly for the antiproton cooling it is crucial to aim at optimum signal to noise ratio at the pickup side.

Cooling of pickup terminators with liquid- N_2 and application of low noise head amplifiers are envisaged. In addition, the mechanical distance between pickup electrodes is planned to be reduced synchronously to the progress of transverse cooling, in order to yield an optimum Schottky signal.

The requirement of a total cooling time of 5 s for antiprotons is considered to be feasible if the "state of the art" achieved at CERN and FNAL is applied adequately to the technical design of the CR cooling system. For rare isotope cooling, the total cooling time of 0.5 s seems to be rather challenging, though the signal to noise ratio for highly charged ions is excellent. Fortunately, the results of cooling experiments at the ESR with

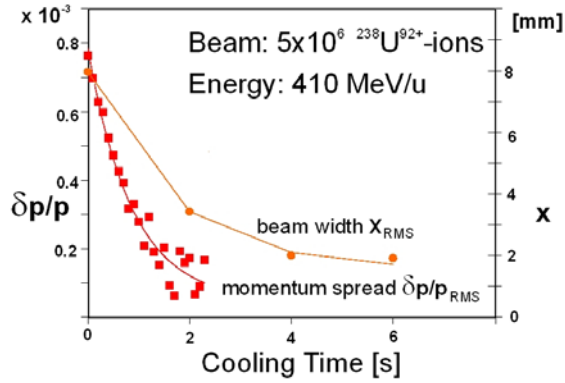


Figure 9: Results of stochastic cooling experiment at ESR (see text).

artificially heated fully stripped uranium ions at 410 MeV/u are quite promising (see fig. 9). Cooling time constants of less than 1 s for momentum cooling and 2 s for horizontal emittance cooling were obtained with about 500 W total power at 50 Ω -kickers in the frequency band 0.9-1.65 GHz.

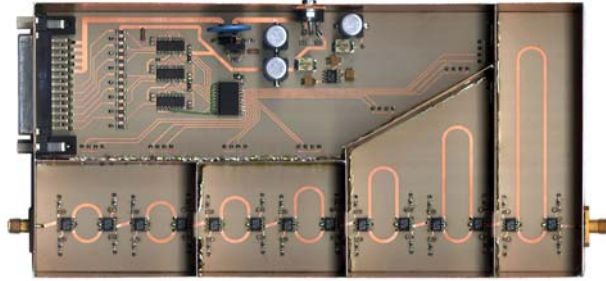


Figure 10: Prototype of a 1.27 ns-delay electronically switched in steps of 10 ps.

So far, we believe that the same pickup and kicker electrodes can be employed for both the RI and the antiproton stochastic cooling. Novel planar electrodes (slit couplers) suitable for the relativistic parameter γ of the beam particles, 1.8 for RI and 4.2 for antiprotons, are under development. The 15% difference in the particle velocities has to be taken into account for the signal combination as well for the electrical length adjustment of transmission lines and notch filters. Suitable electronically switched delay units are under development. A prototype is seen in Figure 10.

6 Beam Accumulation

6.1 Rare Isotope Accumulation

Pre-cooled rare isotope bunches can be transferred either directly or after deceleration in the RESR to a lower specific energy to the NESR. If allowed by the lifetime of nuclei, the rare isotope beams may be accumulated in the NESR by means of RF stacking and electron cooling. This method has been applied successfully for many years at the existing ESR. Achievable stacking factors are proportional to the beam lifetime divided by the time between two subsequent injections. If the latter is assumed to be about 1 s, we may expect stacking factors that are approximately equal to the nuclear decay time of the exotic ions in the laboratory system (see table 2). Hence, e.g. for ^{132}Sn , one could accumulate up to 2.4×10^9 nuclei within one minute. With an internal target of 4×10^{13} atoms/cm² and 1 MHz revolution frequency a luminosity of about 1×10^{29} cm⁻²s⁻¹ would be available for experiments.

6.2 Antiproton Accumulation

After pre-cooling in the CR, single bunches of up to 1×10^8 antiprotons are transferred every 5 s to the accumulator ring RESR, where RF stacking will be combined with stochastic accumulation. The injected bunch is captured into a first harmonic RF bucket, moved towards the tail of the stack and de-bunched there. The momentum cooling into the stack core is made by two or three separate pickup and kicker systems. In addition, the core of the stack has to be cooled all the time in all phase planes. About 7×10^{10} antiprotons per hour shall be accumulated this way. The accumulated antiproton beam are transferred to SIS100 for further acceleration to the energy required for the internal target experiment at the HESR. The design of the RESR, recently added to the storage ring complex, is in a very early stage. The main motivation was, to have a ring especially optimized for the fast accumulation of antiprotons. The lattice is under investigation and the conceptual design of the stochastic accumulation system has just begun. We hope to get, at least, some advice from experts at FNAL and CERN, where similar requirements have been fulfilled many years ago.

7 Electron Cooling Concept

7.1 RI Beams in NESR

Because of the short lifetime of exotic nuclei one has to optimize stochastic pre-cooling in the CR and final electron cooling in the NESR. Stochastic cooling rates decrease strongly when the beam temperatures approach a certain lower limit, where the (wanted) mixing is so slow and the signal to noise ratio so small that the cooling process is stopped. Electron cooling rates show the opposite behavior. They reach optimum values as soon as the longitudinal and transverse beam temperatures are small enough, i.e. the relative velocities between cooling electrons and ions are comparable to the mean electron velocity spread. The envisaged final beam parameters after pre-cooling in the CR may be considered as optimum parameters for the subsequent electron cooling in the NESR, where electron cooling rates between 1 and 10 s^{-1} are required.

Main applications for electron cooling at the NESR are

- fast accumulation of RI beams,
- compensation for beam heating and mean energy loss in the internal target in proton scattering experiments, and
- formation of short ion bunches for the collision with electron bunches for electron scattering experiments, including the compensation for phase space dilution by beam-beam effects.

Main parameters of the NESR electron cooler are:

- 10-450 keV variable electron energy corresponding to electron cooling in the ion energy range 20 to 800 MeV/u,
- up to 2 A electron current at a beam diameter of 25 mm,
- $\leq 0.2 \text{ eV}$ transverse electron temperature,
- about 0.2 T solenoid field in the cooling section with a straightness of $B_{\perp}/B_{\parallel} \leq 5 \times 10^{-5}$, and
- effective cooler length of 4 m.

The rather tight tolerance for the straightness of the magnetic field in the cooling section is absolutely necessary to attain the envisaged cooling rates $\geq 10 \text{ s}^{-1}$, especially at high cooling energies. Numerical simulations using different codes have confirmed

this. Another result of the simulations is the necessity of sufficiently high magnetic field strength, in order to achieve the so-called magnetized cooling delivering much higher cooling rates compared to non-magnetized cooling at lower fields. The simulation results are in fairly good agreement with experimental cooling results at the ESR in a wide range of ion energies up to 450 MeV/u.

7.2 Antiprotons in HESR

Very similar to the situation in the NESR, beam quality and luminosity in the HESR will be determined by the capability to counteract beam heating caused by antiproton-target interactions and by intra-beam scattering. The realization of the technical requirements that can be derived from the experimental experience with electron cooling at lower energies is quite challenging. As mentioned above and confirmed by recently performed numerical simulations strong cooling can be achieved only by magnetized cooling requiring a strong longitudinal magnetic field ($B_{\parallel} \geq 0.5$ T) that guides the electron beam along the entire interaction region of up to 30 m length. It is evident that the requirements concerning the parallelism of the magnetic field ($B_{\perp}/B_{\parallel} \leq 1 \times 10^{-5}$) are even more stringent than for the NESR electron cooler and absolutely mandatory for reasonably high cooling rates (0.1 to 0.01 s⁻¹), especially at the highest antiproton energies between 10 and 14 GeV.

The generation of a cold electron beam at energies up to 8 MeV (corresponding to an antiproton energy of 14 GeV) with an electron current of up to 1 A is another technical challenge. If magnetized cooling with a maximum energy of 8 MeV is required, two possible solutions for the acceleration of the electrons are conceivable: electrostatic acceleration or linear RF accelerator. Electrostatic acceleration certainly has the advantage of small energy spread in the electron beam compared to the acceleration by an RF linac. Moreover, it provides a continuous electron beam without any time structure, which would be best suited for the cooling of a coasting antiproton beam in the HESR.

The acceleration of electron beams in commercially available electrostatic accelerators might be feasible if the electron beam current can be recuperated with high efficiency. An electron current loss below 100 μ A seems to be acceptable in this type of accelerator. First experiments in the framework of a similar research program at FNAL/USA are promising [19], but, so far, the project is not focused to achieve the considerably higher cooling rates by means of magnetized cooling. The technical feasibility of magnetized cooling in the full energy range of the HESR is presently being studied in close cooperation with BINP in Novosibirsk.

References

- [1] An International Accelerator Facility for Beams of Ion and Antiprotons, Conceptual Design Report, GSI (2001)
- [2] P. Spiller et al., Proceedings of the EPAC02, Paris (2002), 626
- [3] A.D. Kovalenko et al., Proceedings of the EPAC02, Paris (2002), 2406
- [4] A.D. Kovalenko et al., IEEE Transactions on Applied Superconductivity, 12, 161, (2002)
- [5] A.D. Kovalenko et al., Superferric Model Dipole Magnet with the Yoke at 80 K for the GSI Future Fast Cycling Synchrotron, Proceedings of Applied Superconductivity Conference, Houston, Texas, **Vol. 13, N2**, 1335 – 1338, (2002)
- [6] I. Koop, V.E. Keilin et al., Conceptual Design of the Superferric Superconducting

- Dipole for the SIS100, Internal GSI Report (2003)
- [7] M.N. Wilson et al., Cored Rutherford Cables for the GSI Fast Ramping Synchrotron, Proceedings of Applied Superconductivity Conference, Houston, Texas, **Vol. 13, N2**, 1704 – 1709, (2002)
- [8] V.E. Keilin and S.S. Kozub, Conceptual Design of the Superferric Superconducting Dipole for the SIS100, Internal GSI Report (2002)
- [9] H. Damerau, M. Emmerling, P. Hülsmann, Vorschlag eines Beschleunigerschemas für die Maschinen SIS12/18 und SIS100 bei GSI, GSI Internal Report (2001)
- [10] A. Krämer et al., Proceedings of EPAC02, Paris (2002), 2547
- [11] O. Gröbner, CAS, Snekersten (1999), 127-138
- [12] P. Spiller, Vorschlag für einen Kollimatorpumpstand zur gezielten Beseitigung von Desorptionsgasen, GSI Internal Report, GSI-SIS-02-02
- [13] Information about Super-FRS and RI production rates taken from [1], p. 145 ff.
- [14] N.A. Tahir et al., Phys. Rev. **E 60**, 4715, (1999)
- [15] H. Koziol and S. Maury, CERN-PS 95-15 (AR/PD) (1995)
- [16] D. Möhl, Hyperfine Interactions **109**, 33, (1997)
- [17] A. Dolinskii et al., Proceedings of the EPAC02, Paris, 2002
- [18] R. Giannini, P. Lefèvre, D. Möhl, Nucl. Phys. **A 558**, 519c (1993)
- [19] J.A. MacLachlan, editor, "*Prospectus for an Electron Cooling System for the Recycler*", Fermilab-TM-2016 (1998).